Progress In Electromagnetics Research B, Vol. 10, 55–74, 2008

STUDY THE EFFECTS OF ELECTROMAGNETIC BAND-GAP (EBG) SUBSTRATE ON TWO PATCHES MICROSTRIP ANTENNA

H. F. Shaban, H. A. Elmikaty, and A. A. Shaalan

Zagazig University
Cairo, Egypt

Abstract—Utilization of electromagnetic band-gap (EBG) structures is becoming attractive in the electromagnetic and antenna community. In this paper, the effects of a two-dimensional electromagnetic band-gap (EBG) Structures on the performance of microstrip patch antenna arrays are investigated using the Ansoft High Frequency Selective Simulator (HFSS$^{\text{TM}}$). A mushroom-like EBG structure is compared with 2-DEBG Structures. HFSS$^{\text{TM}}$ is employed to determine the effects of different Structures on two element microstrip patch antennas array. Two element microstrip patch antenna array on a uniform substrate suffer from strong mutual coupling due to the pronounced surface waves. Therefore, diverse forms of 2-DEBG Structures like: little number of holes, large number of holes, defect mode and different number of mushroom-patches columns structure are discussed. The two element microstrip patch antennas array placed on a defect in the electromagnetic (EBG) substrate that localizes the energy under the antennas. The excitation frequency of the two element microstrip patch antennas array near the resonance frequency of the defect mode can be used to control the coupling between antennas that are placed in an array. The mutual coupling improved by using large number of mushroom-patches columns structure.

1. INTRODUCTION

In recent years, a new technology has emerged which may be the key to developing ultra-wideband microstrip antennas. This technology manipulates the substrate in such a way that surface waves are completely forbidden from forming, resulting in improvements in antenna efficiency and bandwidth, while reducing sidelobes and electromagnetic interference levels. These substrates contain so-called Photonic Crystals. Also known as electromagnetic band-gap (EBG) structures and electromagnetic band-gap materials (EBMs), are a class of periodic metallic, dielectric, or composite structures that exhibit a forbidden band, or bandgap, of frequencies in which waves incident at various directions destructively interfere and thus are unable to propagate [1, 2]. Based on the dimensional periodicity of the crystal structure, the bandgaps can be in one, two, or three-dimensional planes, with the level of complexity increasing as the dimensions increase. The first photonic-crystal structure conceptualized and manufactured was in 1991 by Yablonovitch, then at Bell Communications Research in New Jersey. Yablonovitch fabricated the crystal structure by mechanically drilling holes a millimeter in diameter into a high dielectric constant material [2]. If the periodicity in an EBG structure is perturbed by either removing or adding a material with a different dielectric constant, size, or shape, a "defect" state is created in the forbidden gap, where an electromagnetic mode is allowed, and localization of the energy occurs [3]. This paper focuses the effect of two element microstrip patch antennas array on a uniform substrate and EBG structures. A mushroom-like EBG structure was compared to other EBG structures such as holes, this structure has a winning feature of compactness [4, 5], which is important in communication antenna applications such as filters in microstrip lines [6, 7], as high-power microwave components [8]. This effects realized by using Ansoft HFSS$^{\text{TM}}$ (High Frequency Selective Simulator). Two element microstrip patch antennas array on a uniform substrate suffer from high surface waves, narrow bandwidth and high mutual coupling. EBG structures are simple solutions to the problem of surface waves. If an EBG structures are designed such that the frequencies of the substrate modes fall within the stop band, the excited substrate modes will exponentially decay, hence reducing the energy lost into the substrate and increasing the energy coupled to the radiated field. Yang et al. originally proposed that high-gain antenna structures could be obtained by printing an antenna on a two-dimensional electromagnetic crystal (2-DEBM) [9]. In this work 2-DEBM s are employed as a means of eliminating the substrate and surface modes for patch antennas. In addition, a 2-DEBM antenna structure is fabricated with a defect point in the EBM substrate, placed under the patch location. This point defect is used to localize the field within the defect region, hence, confining the energy under the patch. The energy confinement leads to a more efficient antenna as well as providing a simpler method of fabrication. The remainder of the paper concentrate on reducing the strong mutual coupling of microstrip antennas on a thick and high permittivity substrate, the mushroom-like EBG structure is inserted between antenna elements. When the EBG parameters are properly designed, the pronounced surface waves are suppressed, resulting in a low mutual coupling. This method is compared with previous methods such as cavity back patch antennas. The EBG structure exhibits a better capability in lowering the mutual coupling than those approaches. Finally, several antennas with and without the EBG structure are fabricated on Rogers RT/Duroid 6010 substrates ($\varepsilon_r = 10.2$). The computed results demonstrate the utility of the EBG structure, and this approach is potentially useful for a variety of array applications.

2. BAND GAP CHARACTERIZATION OF THE EBG STRUCTURE

Indeed, the formation of the bandgap is dependent on the periodicity of the crystal, but it is also heavily dependent on the refractive index (dielectric constant) ratios between the base material (the substrate as a whole) and the impurities that form the crystal. Typically, the refractive index ratio must be at least 2 : 1 (substrate-to-impurity) ratio for the bandgap to exist [2]. For the 2-D triangular structure, the broadest bandgap is obtainable when the impurities (the cylindrical post) are of air ($\varepsilon_r = 1$), while the base material is a high dielectric constant (for example, $\varepsilon_r = 10$). A 10 : 1 dielectric (3.16 : 1 refractive index) ratio would satisfy the index requirement and form a broad bandgap, with proper crystal spacings. This explains the need for a high dielectric substrate for a patch antennas designed on a photonic crystal substrate. A photonic crystal essential behaves much like a bandstop filter, rejecting the propagation of energy over a fixed band of frequencies. However, once a defect is introduced such that it disrupts the periodicity in the crystal, an area to localize or "trap" electromagnetic energy is established. In this region, a passband response is created. This ability to confine and guide electromagnetic energy has several practical applications at microwave frequencies as filters, couplers, and especially antennas. This rather simple concept of placing defects in a photonic crystal structure introduces a new methodology in the design of microstrip (patch) antennas. The idea is to design a patch antenna on a 2D photonic crystal substrate, where the patch becomes the "defect" in the crystal structure. In this case, a crystal array of cylindrical air holes are patterned into the dielectric substrate of the patch antenna. By not patterning the area under the patch, a defect is established in the photonic crystal, localizing the EM fields. Surface waves along the XY plane of the patch are forbidden from forming due to the periodicity of the photonic crystal in that plane. This prevention of surface waves improves operational bandwidth and directivity, all while reducing sidelobes and coupling, which are common concerns in microstrip antenna designs. Using these concepts, a photonic crystal patch antenna was developed. The mushroom-like EBG structure was first proposed in [10]. It consists of four parts: a ground plane, a dielectric substrate, metallic patches, and connecting vias. This EBG structure exhibits a distinct stopband for surface-wave propagation. The operation mechanism of this EBG structure can be explained by an LC filter array [11]: the inductor L results from the current flowing through the vias, and the capacitor C due to the gap effect between the adjacent patches. For an EBG structure with patch width W, gap width g, substrate thickness h and dielectric constant ε_r, the values of the inductor L and the capacitor C are determined by the following formula [12]:

$$L = \mu_0 h \tag{1}$$

$$C = \frac{W\varepsilon_0 (1+\varepsilon_0)}{\pi} \cos h \frac{(2W+g)}{g} \tag{2}$$

μ_0 is the permeability of free space and ε_0 is the permittivity of free space. Reference [12] also predicts the frequency band gap as

$$w = \frac{1}{\sqrt{LC}} \tag{3}$$

$$BW = \frac{\Delta w}{w} = \frac{1}{\eta}\sqrt{\frac{L}{C}} \tag{4}$$

where η is the free space impedance which is 120π.

The use of electromagnetic bandgap structure in microstrip antenna is to improve the properties of the antenna parameters [13–15].

3. EFFECTS OF THE EBM SUBSTRATE

3.1. Small Number of Holes

Two pairs of microstrip antennas are fabricated on Roger RT/Duroid 6010 substrates. The permittivity of the substrate is 10.2, and the substrate thickness is 1.92 mm. Each patch size is 6.8 mm × 5 mm, and the spacing between the antennas' edges is 48.4 mm. The patches are fabricated on a ground plane of 100 mm × 50 mm. Fig. 1 shows a photograph of the fabricated antennas with and without the EBG structure. For the EBG structures, triangular lattice with lattice constant of 1.38 cm and a hole diameter of 1.27 cm and was originally designed to have a gap at approximately 5.8 GHz.

The computed results by using HFSS$^{\text{TM}}$ are shown in Fig. 2. It is observed that for the antennas without the EBG structure resonate at 5.86 GHz with return loss better than -10 dB and for the antennas with

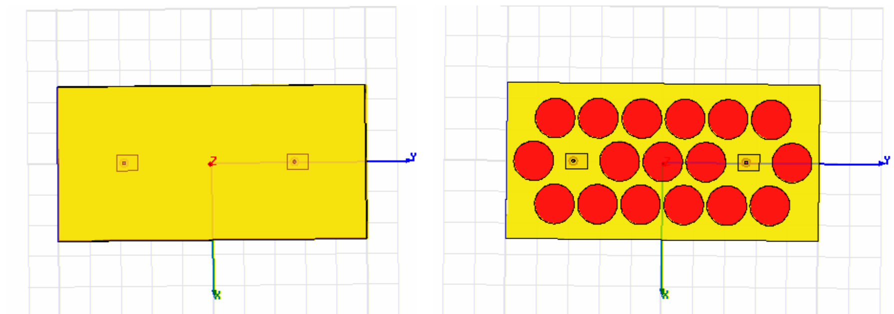

Figure 1. Photo of microstrip antennas with and without the EBG structure. The substrate thickness is 1.92 mm and its dielectric constant is 10.2. The antenna size is 6.8 mm $\times$ 25 mm with a distance of 48.4 mm. The EBG structure triangular lattice with lattice constant of 1.38 cm and a hole diameter of 1.27 cm.

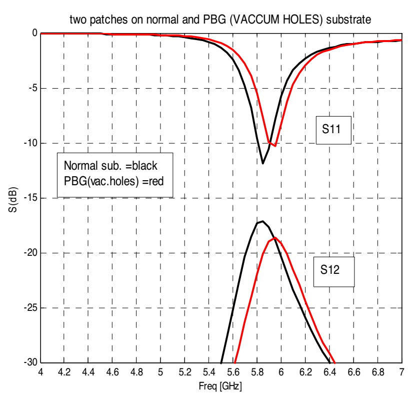

Figure 2. Computed results of microstrip antennas with and without the EBG structure. An 2 dB mutual coupling reduction is observed at the resonant frequency.

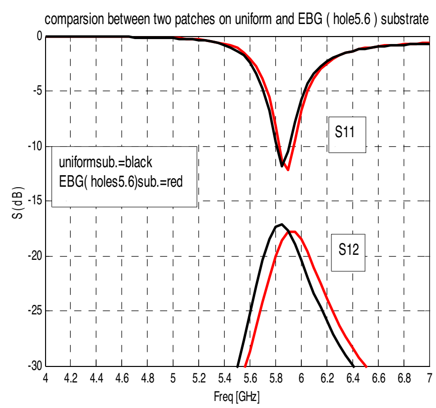

Figure 3. Computed results of microstrip antennas with and without the EBG structure. An 1 dB mutual coupling reduction is observed at the resonant frequency.

the EBG structure of vacuum holes resonate at 5.96 GHz with return loss little better than −10 dB. The mutual coupling of the antennas without the EBG structure is −16.8 dB. In comparison, the mutual coupling of the patches with the EBG structure is only −18.9 dB. An approximately 2 dB reduction of mutual coupling is achieved. To investigate the effects of a EBG structure as in the previous case is used, but now the hole are filled with a material instead of air with dielectric constant of 5.6.

The computed results by using HFSS$^{\text{TM}}$ are shown in Fig. 3. It is observed that for the antennas with the EBG structure of holes (5, 6) was resonate at 5.92 GHz with return loss better than −10 dB, and the mutual coupling of the antennas with the EBG structure is −17.8 dB. An approximately 1 dB reduction of mutual coupling is achieved. Also, to investigate the effects of a EBG structure as in the previous cases are used, but now the hole are filled with a material with dielectric constant of 10.6. The computed results by using HFSS$^{\text{TM}}$ are shown in Fig. 4. It is observed that for the antenna with the EBG structure of holes (10.6) resonate at 5.9 GHz with return loss better than −10 dB. With mutual coupling with the EBG structure is −16.85 dB. We can compare the computed results between the uniform and EBG substrate (holes of 5.6 and 10.6) in Fig. 5, it is observed that for the antennas with and without the EBG structure of holes have return loss better than −10 dB. With mutual coupling with the EBG structure is improved by small values.

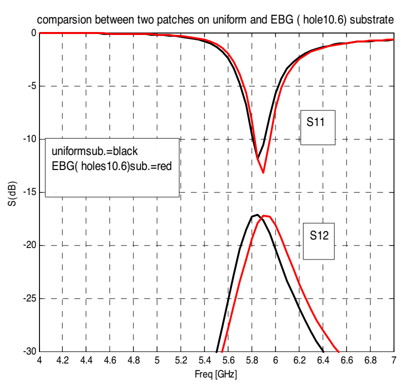

Figure 4. Computed results of microstrip antennas with and without the EBG structure. An 0.05 dB mutual coupling reduction is observed at the resonant frequency.

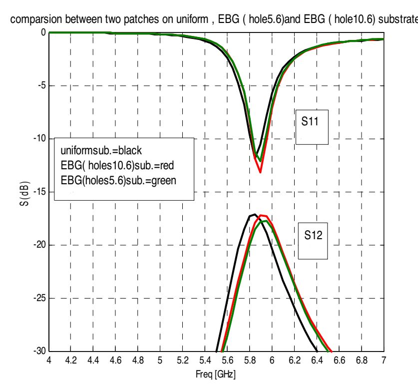

Figure 5. Computed results of microstrip antennas with and without the EBG structure. Mutual coupling improved by very small values at the resonant frequency.

To investigate the effects of a EBG structure as in the previous cases by change only the kind of the material of middle holes of the structure with dielectric constant of 5.6 and 10.6 value, Fig. 6 shows a photograph of the fabricated antennas with the EBG structure. The computed results by using HFSS$^{\mathrm{TM}}$ are shown in Fig. 7 the mutual coupling between patches with the EBG structure at the resonant frequency is not improved.

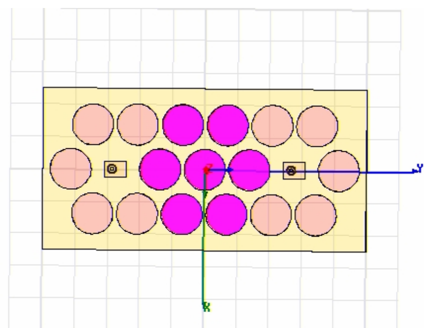

Figure 6. Photo of microstrip antennas with the EBG structure.

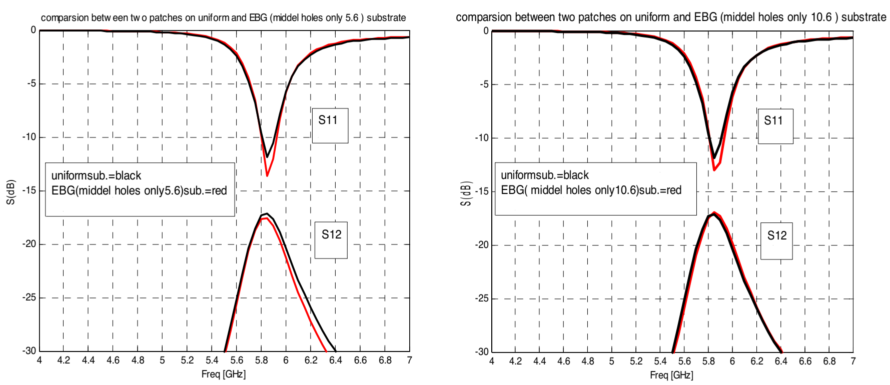

(a) (b)

Figure 7. Computed results of microstrip antennas with and without the EBG structure. mutual coupling is not improved at the resonant frequency.

By changing the materials of the holes (porcelain holes with dielectric constant of 5.7 around the patches and vacuum in the middle holes) as in Fig. 8. The computed results by using HFSS$^{\mathrm{TM}}$ are shown in Fig. 9 with mutual coupling improved by small values (1 dB).

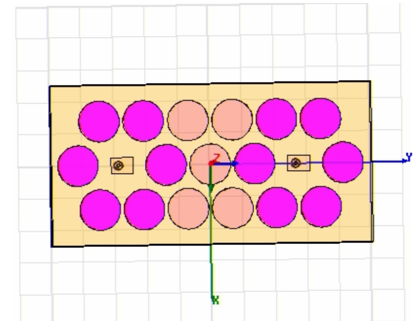

Figure 8. Photo of microstrip antennas with the EBG structure (porcelain holes of 5.7 around the patches and vacuum in the middle holes).

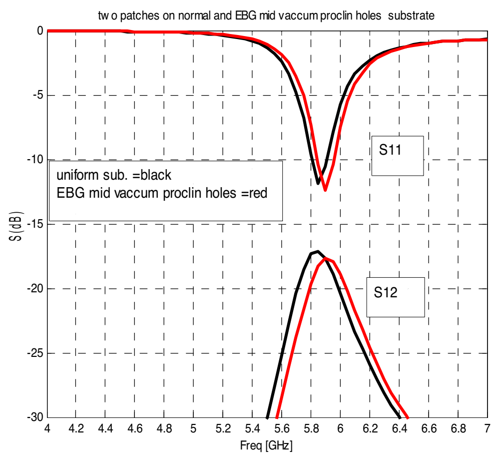

Figure 9. Computed results of microstrip antennas with and without the EBG structure. An 1 dB mutual coupling reduction is observed at the resonant frequency.

To simplify the EBG structure as in the previous cases by change the structure of holes between the patches with dielectric constant of 5.6 and 10.6 values, Fig. 10 shows a photograph of the fabricated antennas with the EBG structure. The computed results by using HFSS$^{\mathrm{TM}}$ are shown in Fig. 11, the mutual coupling with the EBG structure is improved by small value.

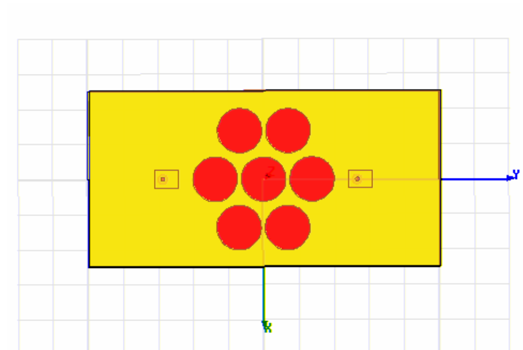

Figure 10. Photo of microstrip antennas with simplify EBG structure.

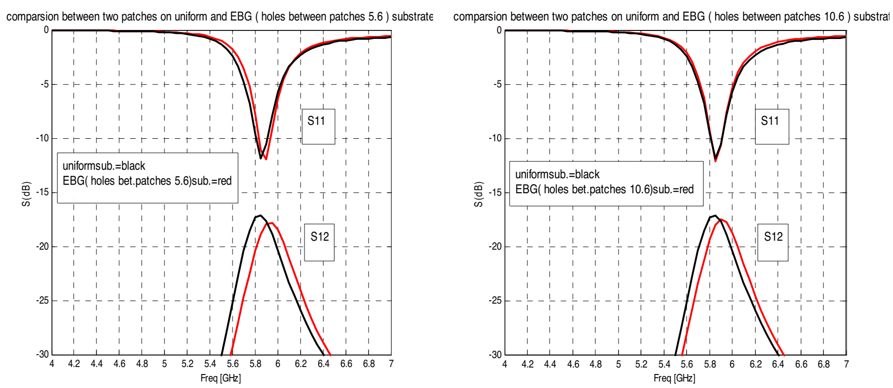

(a) (b)

Figure 11. Computed results of microstrip antennas with and without simplify EBG structure. Mutual coupling is improved by small values at the resonant frequency.

3.2. Large Number of Holes

Two pairs of microstrip antennas are fabricated on Roger RT Duroid 6010 substrates. The permittivity of the substrate is 10.2, and the substrate thickness is 1.92 mm. The antenna's size is 6.8 mm × 5 mm, and the distance between the antennas' edges is 48.4 mm. The antennas are fabricated on a ground plane of 150 mm × 100 mm. Fig. 12 shows a photograph of the fabricated antennas with and without the EBG structure. For the EBG structures, triangular lattice with lattice constant of 1.38 cm and a hole diameter of 1.27 cm and was originally designed to have a gap at approximately 5.8 GHz.

The computed results by using HFSS$^{\text{TM}}$ are shown in Fig. 13. The mutual coupling with the EBG structure is improved by 2 dB at the resonant frequency. Then, to investigate the effects of a EBG structure as in the previous cases are used, but now the holes are filled

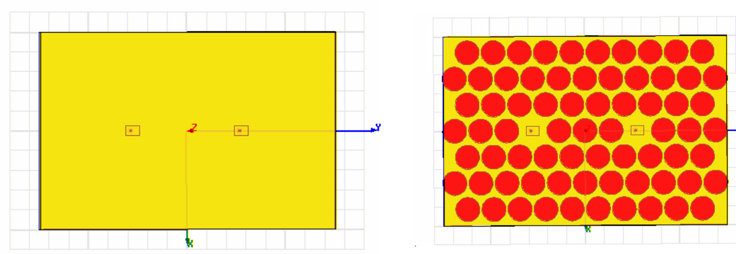

Figure 12. Photo of microstrip antennas with and without the EBG structure. The substrate thickness is 1.92 mm and its dielectric constant is 10.2. The antenna size is 6.8 mm × 25 mm with a distance of 48.4 mm. The EBG structure triangular lattice with lattice constant of 1.38 cm and a hole diameter of 1.27 cm.

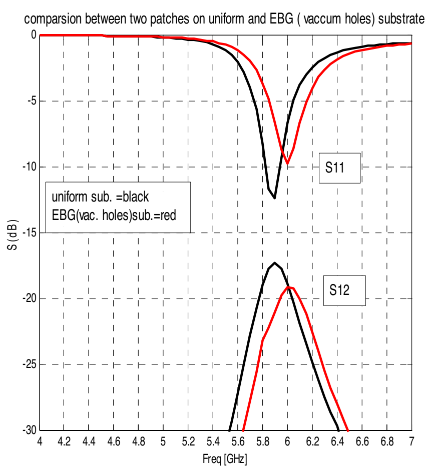

Figure 13. Computed results of microstrip antennas with and without simplify EBG structure. An 2 dB mutual coupling reduction is observed at the resonant frequency.

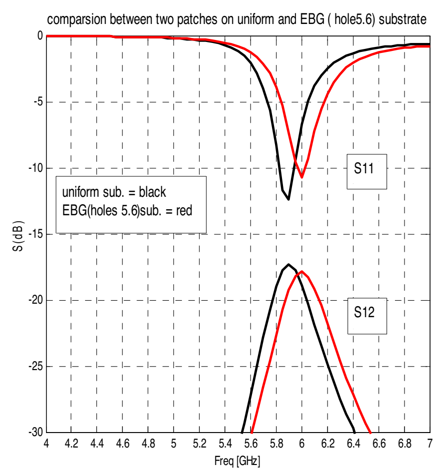

Figure 14. Computed results of microstrip antennas with and without simplify EBG structure. An 1 dB mutual coupling reduction is observed at the resonant frequency.

of a material with dielectric constant of 5.6 and 10.6. The computed results by using HFSS$^{\text{TM}}$ are shown in Fig. 14 and Fig. 15.

3.3. Defect Mode

A defect state is created in the forbidden gap where an electromagnetic mode is allowed and localization of the energy occurs [3]. A 2-DEBG antenna structure is fabricated with a defect point in the EBG substrate, placed under the patch location. This point defect is used to localize the field within the defect region, hence, confining the energy under the patch. The energy confinement leads to a more efficient antenna as well as providing a simpler method of fabrication. For small number of holes to investigate the effects of a EBG structure as in the previous cases are used, but now with defect with dielectric constant of 10.6. Fig. 17 shows Photo of microstrip antennas with horizontal and vertical defect EBG structure (defect size of 5 mm × 8 mm). The computed results by using HFSS$^{\text{TM}}$ are shown in Fig. 18. The presence of a point defect under the patch, allows a higher concentration of electromagnetic energy density within the cavity formed by the patch and the fact that the antenna leakage can simply be controlled by tuning to or away from a defect resonance line, and can be used

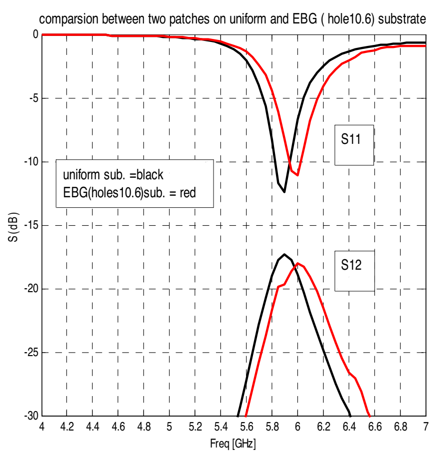

Figure 15. Computed results of microstrip antennas with and without simplify EBG structure. An 2 dB mutual coupling reduction is observed at the resonant frequency.

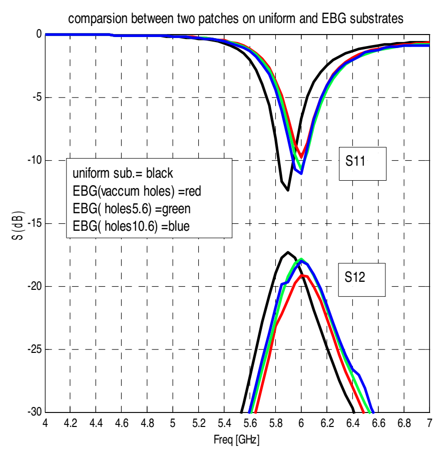

Figure 16. Computed results of microstrip antennas with and without simplify EBG structure. Comparison between normal and EBG substrates.

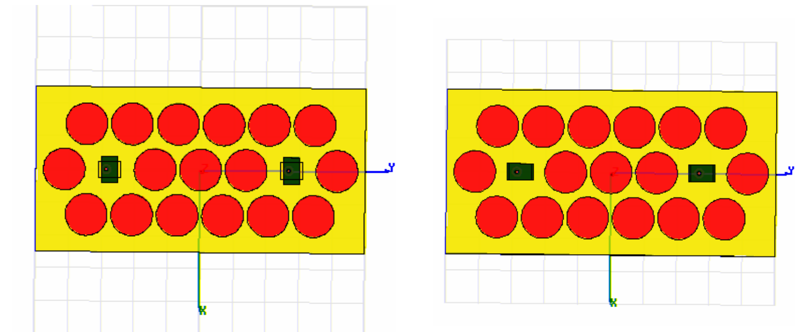

Figure 17. Photo of microstrip antennas with horizontal and vertical defect EBG structure. The substrate thickness is 1.92 mm and its dielectric constant is 10.2. The antenna size is 6.8 mm × 25 mm with a distance of 48.4 mm. The EBG structure triangular lattice with lattice constant of 1.38 cm and a hole diameter of 1.27 cm. Defect size is 5 mm × 8 mm.

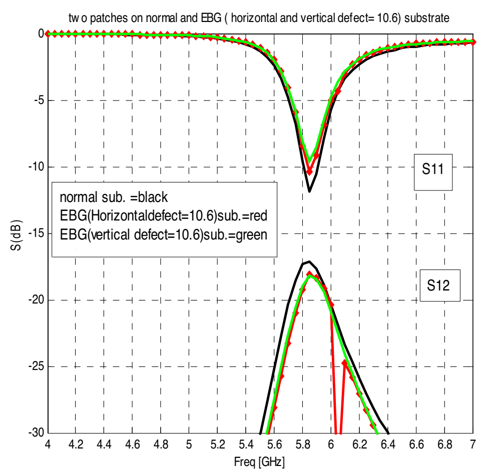

Figure 18. Computed results of microstrip antennas with and without simplify EBG structure. Comparison between normal and EBG substrates with horizontal and vertical defect with dielectric constant of 10.6.

to inhibit or stimulate the coupling between different elements of a microstrip patch antennas array. Also, to investigate the effects of a EBG structure as in the previous cases are used, but now the middle holes are filled with a material with dielectric constant of 10.6. Photo of microstrip antennas with horizontal defect and the computed results of horizontal defect (size of 5 mm × 8 mm) by using HFSS$^{\text{TM}}$ are shown in Fig. 19.

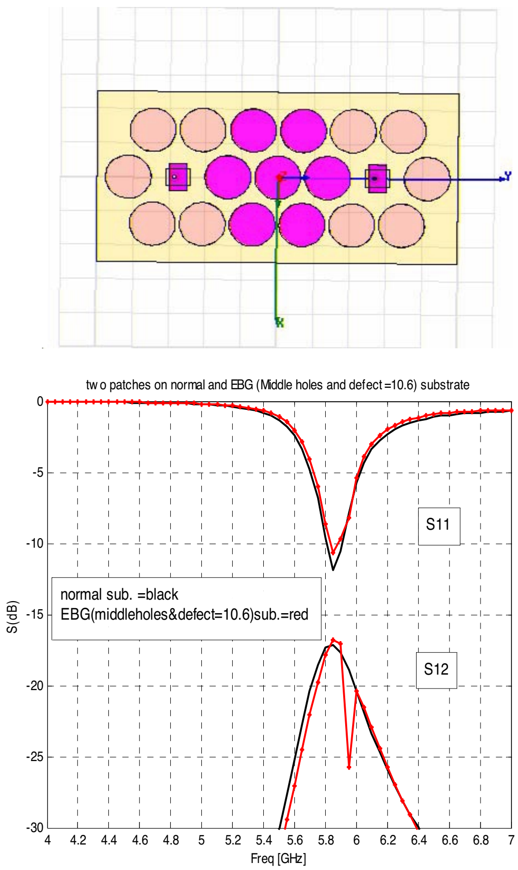

Figure 19. Photo of microstrip antennas with horizontal defect and the Computed results of microstrip antennas with and without simplify defect EBG structure. Comparison between normal and EBG substrates with horizontal defect with dielectric constant of 10.6.

For large number of holes, to investigate the effects of a EBG structure as in the previous cases are used, but now with defect with dielectric constant of 10.6. Fig. 20 shows Photo of microstrip antennas with horizontal and vertical defect EBG structure (defect size of 5 mm × 8 mm). The computed results by using HFSS^{TM} are shown in Fig. 21.

But by changing the defect with dielectric constant of 5.6, the computed results by using HFSS^{TM} are shown in Fig. 22.

For microstrip patch antennas array, the excitation frequency is

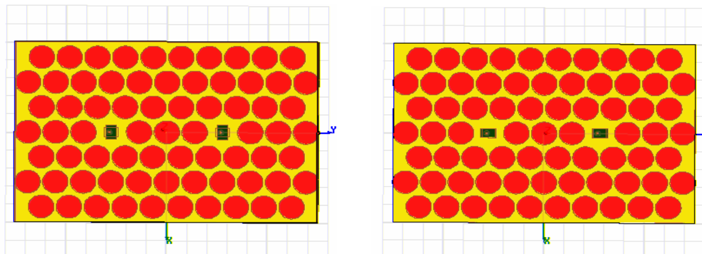

Figure 20. Photo of microstrip antennas with horizontal and vertical defect EBG structure. The substrate thickness is 1.92 mm and its dielectric constant is 10.2. The antenna size is 6.8 mm × 25 mm with a distance of 48.4 mm. The EBG structure triangular lattice with lattice constant of 1.38 cm and a hole diameter of 1.27 cm. Defect size is 5 mm × 8 mm.

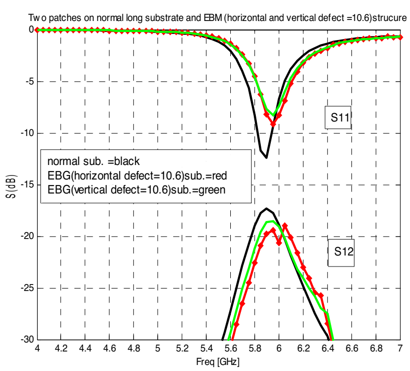

Figure 21. Computed results of microstrip antennas with and without simplify EBG structure. Comparison between normal and EBG substrates with horizontal and vertical defect with dielectric constant of 10.6.

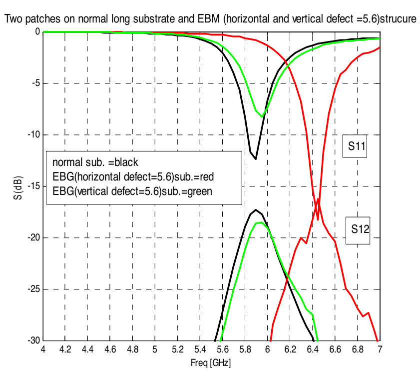

Figure 22. Computed results of microstrip antennas with and without simplify EBG structure. Comparison between normal and EBG substrates with horizontal and vertical defect with dielectric constant of 5.6.

tuned to the horizontal defect. On the other hand, since the excitation frequency is away from the vertical resonance, and yet within the stop band of the 2-DEBG substrate. As we increase the dielectric constant of the defect, the mutual coupling will be improved and tuned to the resonance frequency as in Fig. 21.

3.4. Mushroom-like EBG Structure

Two pairs of microstrip antennas are fabricated on Roger RT/Duroid 6010 substrates. The permittivity of the substrate is 10.2, and the substrate thickness is 1.92 mm. The antenna's size is 6.8 mm × 5 mm, and the distance between the antennas' edges is 38.8 mm. The antennas are fabricated on a ground plane of 100 mm × 50 mm. Fig. 23 shows a photograph of the fabricated antennas with and without the EBG structure. For the EBG structures [11], the mushroom-like patch size is 3 mm and the gap between the patches is 0.5 mm. Four columns of mushroom-like patches are inserted between the antennas and was originally designed to have a gap at approximately 5.8 GHz.

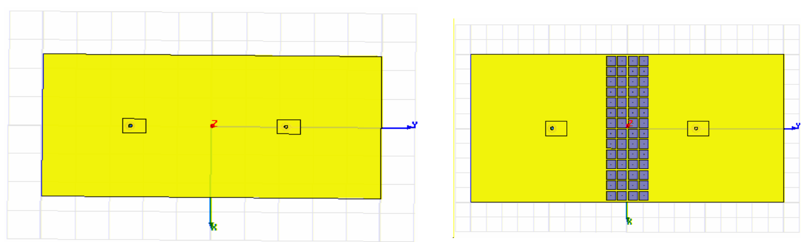

Figure 23. Photo of microstrip antennas with and without the EBG structure. The substrate thickness is 1.92 mm and its dielectric constant is 10.2. The antenna size is 6.8 mm × 5 mm with a distance of 38.8 mm. The EBG mushroomlike patch (4 coln.) size is 3 mm and the gap width is 0.5 mm.

The computed results by using HFSS^{TM} are shown in Fig. 24. It is observed that both antennas have return loss better than −10 dB. For the antennas without the EBG structure, the mutual coupling is −18.5 dB. In comparison, the mutual coupling of the antennas with the EBG structure is only −22.5 dB.

The effect of The EBG mushroom-like patch can be realized by using different number of mushroom-like patch columns (odd and even), firstly we compare the different number of mushroom-like patch structure for odd number of columns. Fig. 25 shows a photograph of the fabricated antennas with and odd number of columns of EBG

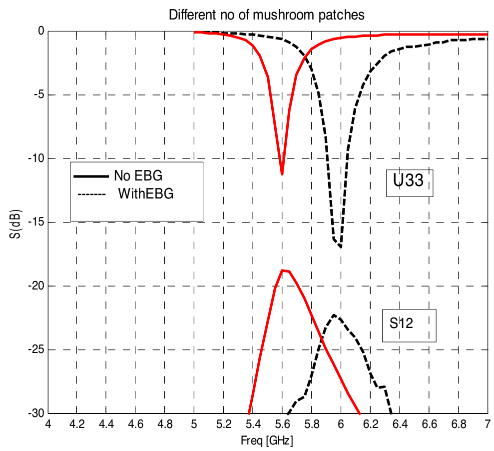

Figure 24. Computed results of microstrip antennas with and without the EBG structure. An 4 dB mutual coupling reduction is observed at the resonant frequency.

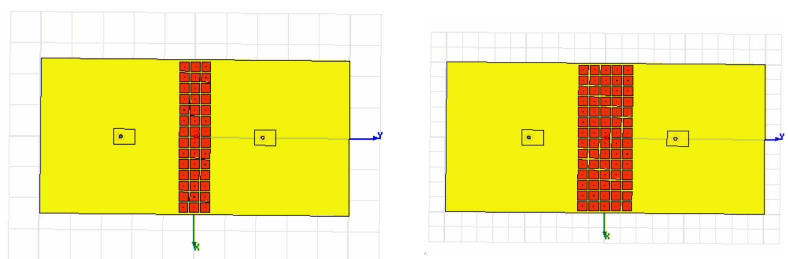

Figure 25. A photograph of the fabricated antennas with and odd number of columns of EBG structure (3 coln. and 5 coln.).

structure. The computed results by using HFSS^{TM} are shown in Fig. 26. It is observed that for the antennas without the EBG structure, the mutual coupling is -18.5 dB. In comparison, the mutual coupling of the antennas with the EBG structure (3 coln.) is -19.8 dB while the EBG structure (5 coln.) only -23.5 dB.

Secondly, we compare the different number of mushroom-like patch structure for even number of columns. Fig. 27 shows a photograph of the fabricated antennas with and even number of columns of EBG structure. The computed results by using HFSS^{TM} are shown in Fig. 28. It is observed that for the antennas without the EBG structure, the mutual coupling is -18.5 dB. In comparison,

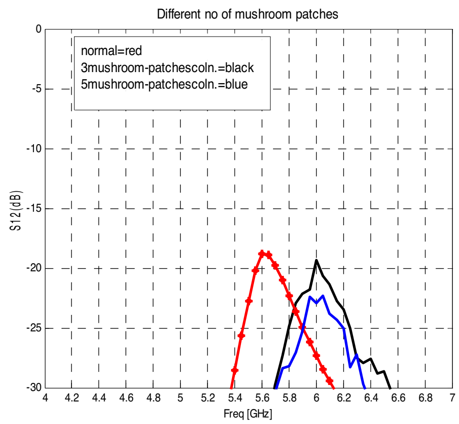

Figure 26. Computed results of microstrip antennas with and without different EBG structure. An 5 dB mutual coupling reduction is observed at the resonant frequency for 5 coln. of mushroom-like patch structure.

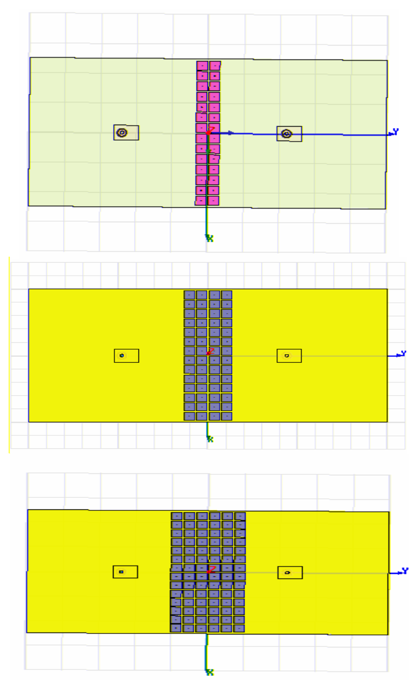

Figure 27. A photograph of the fabricated antennas with and even number of columns of EBG structure (2 coln., 4 coln., and 6 coln.).

the mutual coupling of the antennas with the EBG structure (2 coln.) is −19.2 dB while the EBG structure (4 coln.) only −22.5 dB and the EBG structure (6 coln.) only −23.5 dB. From this computed demonstration, it can be concluded that the EBG structure can be utilized to reduce the antenna mutual coupling between array elements. The reduction of mutual coupling improved by increasing number of columns of mushroom-like patches structure. Fig. 29 demonstrated the effect of different number of columns on the mutual coupling of microstrip patch antennas array by using HFSS^{TM}.

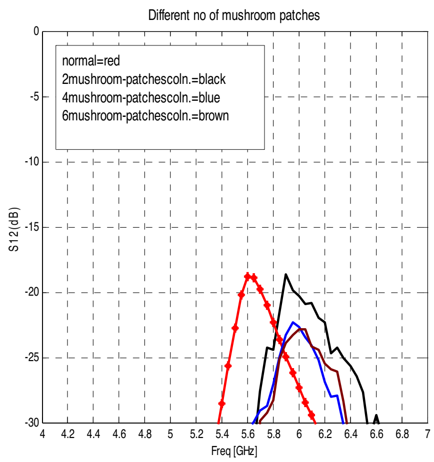

Figure 28. Computed results of microstrip antennas with and without different EBG structure. An 5 dB mutual coupling reduction is observed at the resonant frequency for 6 coln. of mushroom-like patch structure.

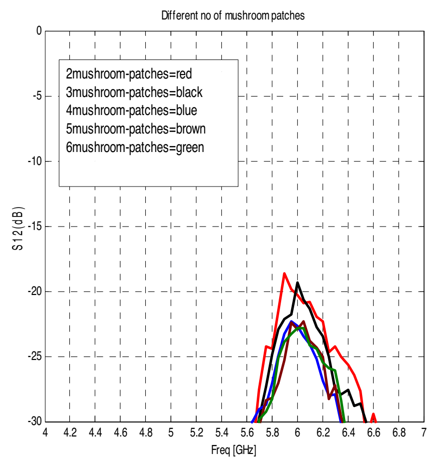

Figure 29. Computed results of microstrip antennas with different EBG structure. An 5 dB mutual coupling reduction is observed at the resonant frequency for 6 coln. of mushroom-like patch structure.

4. CONCLUSION

A 2-DEBG structure was integrated with two element of microstrip patch antennas array. The properties of this structure and the effects of the substrate were studied using a HFSS^{TM} code. It is instructive to compare the normal structure with other EBG structures used to reduce the mutual coupling. During the comparison, the antenna size, substrate properties, and antenna distance in all the structures are kept the same as in the normal case. The normal microstrip antennas show the highest mutual coupling. The small number of holes case and the large number of holes case have some effects on reducing the mutual coupling. A 1.5 dB mutual coupling reduction is noticed for the former case and a 2 dB reduction is observed for the latter case. The presence of the defect under the patch can increase the radiated power due to the energy storage under the antenna and a 3.5 dB mutual coupling reduction is noticed for the defect mode. The lowest mutual coupling is obtained in the mushroom-like patches structure case as a 5 dB reduction is achieved. On the other hand, the mushroom-like patches structure is more expensive than the other approaches. This comparison demonstrates the EBG structure can be utilized to reduce the antenna mutual coupling between array elements and the antenna leakage can simply be controlled by tuning to or away from a defect resonance line, can be used to inhibit or stimulate the coupling between different elements of microstrip patch antennas array. Therefore, incorporating point defects in a 2-DEBG substrate for microstrip patch antennas array also present itself as a viable approach in designing more efficient antenna arrays.

REFERENCES

1. Agi, K., K. J., Malloy, E. Schamiloglu, M. Mojahedi, and E. Niver, "Integration of a microstrip patch antenna with a two-dimensional photonic crystal substrate," *Electromagnetics*, Vol. 19, 277–290, 1999.
2. Parker, G. and M. Charlton, "Photonic crystals," *Physics World*, Vol. 13, 29–34, Aug. 2000.
3. Joannopoulos, J. D., R. D. Meade, and J. Winn, *Photonic Crystals: Molding the Flow of Light*, Princeton University Press, Princeton, N.J., 1995.
4. Yang, F. and Y. Rahmat-Samii, "Step-like structure and EBG structure to improve the performance of patch antennas on high dielectric substrate," *Proc. IEEE AP-S Dig.*, Vol. 2, 482–485, July 2001.
5. Gonzalo, R., P. Maagt, and M. Sorolla, "Enhanced patch-antenna performance by suppressing surface waves using photonic-bandgap substrates," *IEEE Trans. Microwave Theory Tech.*, Vol. 47, 2131–2138, Nov. 1999.
6. Radisic, V., Y. X. Qian, R. Coccioli, and T. Itoh, "Novel 2-D photonic bandgap structure for microstrip lines," *IEEE Microwave and Guided Wave Letters*, Vol. 8, 69–71, 1998.
7. Rumsey, I., M. Piket May, and P. K. Kelly, "Photonic bandgap

structures used as filters in microstrip circuits," *IEEE Microwave and Guided Wave Letters*, Vol. 8, 336–338, 1998.
8. Agi, K., L. D. Moreland, E. Schamiloglu, M. Mojahedi, K. J. Malloy, and E. R. Brown, "Photonic crystals: A new quasi-optical component for high-power microwaves," *IEEE Transactions on Plasma Science*, Vol. 24, 1067–1071, 1996.
9. Yang, H. Y. D., N. G. Alexopoulos, and E. Yablonovitch, "Photonic band-gap materials for high-gain printed circuit antennas," *IEEE Transactions on Antennas and Propagation*, Vol. 45, 185–187, 1997.
10. Sievenpiper, D., L. Zhang, R. F. J. Broas, N. G. Alexopolus, and E. Yablonovitch, "High-impedance electromagnetic surfaces with a forbidden frequency band," *IEEE Trans. Microwave Theory Tech.*, Vol. 47, 2059–2074, Nov. 1999.
11. Yang, F. and Y. Rahmat Sami, "The effects of an electromagnetic bandgap (EBG) structure on two element microstrip patch antenna array," *IEEE Transactions Antennas and Propagation*, Vol. 51, No. 10, 2936–2946, Oct. 2003.
12. Sievenpiper, D. F., "High-impedance electromagnetic surfaces," Ph.D. dissertation, UCLA, 1999.
13. Chang, C., Y. Qian, and T. Itoh, "Analysis and applications of uniplanar compact photonic bandgap structures," *Progress In Electromagnetic Research*, PIER 41, 211–235, 2003.
14. Xu, H. J., Y. H. Zhang, and Y. Fan, "Analysis of the connection between K connector and microstrip with electromagnetic bandgap (EBC) structures," *Progress In Electromagnetic Research*, PIER 73, 239–247, 2007.
15. Pirhadi, A., M. Hakkak, and F. Keshmiri, "Using electromagnetic bandgap superstrate to enhance the bandwidth of probe FED microstrip antenna," *Progress In Electromagnetic Research*, PIER 61, 215–230, 2006.